STEM CELLS®

TISSUE-SPECIFIC STEM CELLS

Mitochondria Determine the Differentiation Potential of Cardiac Mesoangioblasts

NURIA SAN MARTIN,[a] ANA M. CERVERA,[a] CLAUDIA CORDOVA,[a] DIEGO COVARELLO,[b] KENNETH J. MCCREATH,[a] BEATRIZ G. GALVEZ[a]

[a]Centro Nacional de Investigaciones Cardiovasculares (CNIC), Madrid, Spain; [b]Stem Cell Research Institute, San Raffaele Hospital, Milano, Italy

Key Words. Adult stem cells • Cardiac diseases • Differentiation • Proliferation • Mitochondria

ABSTRACT

An understanding of cardiac progenitor cell biology would facilitate their therapeutic potential for cardiomyocyte restoration and functional heart repair. Our previous studies identified cardiac mesoangioblasts as precommitted progenitor cells from the postnatal heart, which can be expanded in vitro and efficiently differentiated in vitro and in vivo to contribute new myocardium after injury. Based on their proliferation potential in culture, we show here that two populations of mesoangioblasts can be isolated from explant cultures of mouse and human heart. Although both populations express similar surface markers, together with a panel of instructive cardiac transcription factors, they differ significantly in their cellular content of mitochondria. Slow dividing (SD) cells, containing many mitochondria, can be efficiently differentiated with 5-azacytidine (5-aza) to generate cardiomyocytes expressing mature structural markers. In contrast, fast dividing (FD) mesoangioblasts, which contain decreased quantities of mitochondria, do not respond to 5-aza treatment. Notably, increasing mitochondrial numbers using pharmacological nitric oxide (NO) donors reverses the differentiation block in FD mesoangioblasts and leads to a progressive maturation to cardiomyocytes; conversely decreasing mitochondrial content, using respiratory chain inhibitors and chloramphenicol, perturbs cardiomyocyte differentiation in SD populations. Furthermore, isolated cardiac mesoangioblasts from aged mouse and human hearts are found to be almost exclusively mitochondria-low FD populations, which are permissive for cardiomyocyte differentiation only after NO treatment. Taken together, this study illustrates a key role for mitochondria in cardiac mesoangioblast differentiation and raises the interesting possibility that treatments, which increase cellular mitochondrial content, may have utility for cardiac stem cell therapy. STEM CELLS *2011;29:1064–1074*

Disclosure of potential conflicts of interest is found at the end of this article.

INTRODUCTION

Embryonic stem cells (ESCs) and, more recently, induced pluripotential stem cells (iPSCs) are frequently considered appealing progenitor cell types for regenerative medicine programs including functional heart repair [1, 2], as they provide an almost limitless supply of starting material for the generation of particular lineages such as mesodermal cardiac precursors [2, 3]. On the other hand, adult stem cells, a collective term for postnatal cells found in particular organ-specific niches, present a viable alternative to the ESC/iPSC platform [4] and could potentially provide autologous repair. Arguably, the most explored source of these adult stem cells is the bone marrow, which can give rise to progenitor cells of the hematopoietic, endothelial, and mesenchymal lineage [5, 6]. Recently, the existence of resident cardiac progenitor cell populations with stem cell properties has been demonstrated independently in several laboratories [7–9], and, together with ESCs, these populations are currently being explored for their utility in cell replacement strategies [10]. However, as with all potential precursor-cell therapy, the molecular mechanisms that govern differentiation and repair are still poorly understood.

A characteristic feature of cardiomyocytes is their large and intricate network of mitochondria, which are required to coordinate energy demands (ATP generation), calcium homeostasis, and maintain mechanical function throughout the life of the heart [11]. Indeed, this attribute has been exploited recently to provide a nongenetic approach for the isolation of cardiomyocytes from complex cell populations in vitro, by virtue of their large mitochondrial content [12]. Interestingly, mitochondrial function is also suggested to be important during the process of cardiomyocyte differentiation per se [13, 14], as respiratory chain poisoning of ESCs inhibits cardiac muscle generation through mechanisms that have been shown to require a functioning Complex III [15]. Moreover, reactive oxygen species (ROS), either from mitochondrial origin [14] or generated from the nonphagocytic NADPH oxidase family [16], have particular relevance as signaling

Author contributions: N.S.M., A.M.C., C.C., and D.C.: collection and assembly of data; data analysis and interpretation; K.J.M. and B.G.G.: conception and design; data analysis and interpretation; manuscript writing; final approval of manuscript.

Correspondence: Beatriz G. Galvez, Ph.D., Centro Nacional de Investigaciones Cardiovasculares, C/Melchor Fernández Almagro, 3., 28029-Madrid. Spain. Telephone: +34-91-453-1200 (3317); Fax: +349-1453-1240; e-mail: bgonzalez@cnic.es Received December 1, 2010; accepted for publication April 11, 2011; first published online in STEM CELLS *EXPRESS* May 4, 2011.
1066-5099/2009/$30.00/0 doi: 10.1002/stem.654

molecules during ESC differentiation to the cardiomyocyte lineage.

Previously, we demonstrated that a cardiac stem cell population, which we have termed cardiac mesoangioblasts, could be efficiently isolated from both mouse and human adult hearts [7, 17] and are distinct from other reported cardiac stem cells [8, 9]. Although self-renewable, cardiac mesoangioblasts appear precommitted to the cardiac lineage and can engraft into damaged myocardium and form well-structured cardiomyocytes [7, 17]. Considering the potential clinical applications of cardiac progenitor cells as therapeutics, we have further investigated the characteristics of these populations. While isolating multiple mesoangioblast clones from cardiac explants, we observed that two clonal populations were recovered with dissimilar proliferative capacity. We report here that precommitted and fast dividing (FD) mesoangioblasts do not form structural cardiomyocytes upon differentiation, whereas slow dividing (SD) mesoangioblasts populations are capable of upregulating a range of structural cardiac proteins upon differentiation. Analysis of the two mesoangioblasts populations suggests mitochondrial load as an important parameter for commitment to cardiogenesis.

Materials and Methods

Reagents

Unless stated otherwise, all reagents were purchased from Sigma Chemical Company (Sigma-Aldrich, St. Louis, MO, http://www.sigmaaldrich.com). MitoTracker Green, tetramethylrhodamine methyl ester (TMRM), and JC-1 reagents and the Alexa-488 labeling kit were purchased from Molecular Probes (Invitrogen, Carlsbad, CA, http://www.invitrogen.com). Antibodies for flow cytometry analysis CD44, CD34, and CD45, were purchased from BD Biosciences (San Jose, CA, http://www.bdbiosciences.com/eu) and alkaline phosphatase (AP) and CD31 were purchased from ID Labs Inc (London, Ontario, http://www.idlabs.com).

Cell Isolation, Culture, and Differentiation

Cardiac explants from mouse and humans were collected following local guidelines (San Raffaele Hospital, Milano, Italy) after approval by the ethics review board. Mice were treated following the U.S. NIH guidelines, and experiments with human samples conformed to the declaration of Helsinki. Murine and human cardiac mesoangioblasts were isolated from ventricle explants as reported previously [7, 17].

For measurement of proliferation, cells were plated at a density of 1×10^4 cells per square centimeter in complete Dulbecco's modified Eagle medium (DMEM) containing 20% fetal bovine serum (FBS) in the presence or absence of the different agents throughout the whole course and passed every 3 days. At each passage, the number of cells were counted manually from triplicate samples. Population doublings (PDs) were determined by the formula $PD = (\log Nf - \log Ni)/\log_2$, where Nf is number of counted cells and Ni number of seeded cells. Statistical analysis was performed as indicated (t test, $p < .05$). For the induction of differentiation, mesoangioblasts were cultured in DMEM/F12 medium containing 10% FBS with 10 μM azacytidine for 2–5 days. Cells were then harvested as indicated and processed for further analysis.

Cell viability was measured using an MTT assay kit from Sigma. Briefly, at the end of each treatment, plates were removed from the incubator into a laminar flow hood where the medium was replaced with 100 μl fresh medium and 10 μl tetrazodium salt before returning to the incubator for 4 hours, followed by the addition of 100 μl MTT solvent. The plates were left overnight in the dark at room temperature (RT). They were then measured in an enzyme-linked immunosorbent assay plate reader (Labdesign AB, Täby, Sweden, www.pharmaceuticals1.com) at 570 and 690 nm for subtracting background absorbance. The percentages of viable cells were calculated from a standard curve prepared from serial dilutions.

Gene Expression Profiling

Total RNA was isolated in cells with TRIzol reagent (Invitrogen) and reverse transcribed with Taqman (Platinum Taq DNA polymerase, Invitrogen). Real-time quantitative reverse-transcription polymerase chain reaction (qRT-PCR) was performed using the primers described previously [7]. Total genomic DNA was purified using Qiagen DNeasy Tissue Spins (Qiagen, Hilden, Germany, www.qiagen.com). For measurement of mitochondrial DNA (mtDNA), the ratio of mtDNA to nuclear DNA (nDNA) was measured by RT-PCR using the Platinum SYBR Green qPCR SuperMix UDG kit (Invitrogen), and the following primers: mouse *Mt-Co2* (Fw CTACAAGACGCCACAT; Rw GAGAGGGGAGAGCAAT); human *Mt-Co2* (Fw CGATCCCTCCCTTACCATCA; Rw CCGTAGTCGGTGTACTCGTAGGT); mouse *SdhA* (Fw TACTACAGCCCCAAGTCT; Rw TGGACCCATCTTCTATGC); human *SdhA* (Fw TCTCCAGTGGCCAACAGTGTT; Rw GCCCTCTTG TTCCCATCAAC).

Immunoblotting and Immunocytochemistry

Cells were lysed directly on ice in Laemmli buffer and separated by sodium dodecyl sulfate–polyacrylamide gel electrophoresis under reducing conditions. Proteins were blotted to nitrocellulose membranes (Hybond-ECL, Amersham Biosciences, Piscataway, NJ; http://www.gelifesciences. com) followed by incubation with the indicated antibodies. For collection of extracellular matrix (ECM), cells were washed in phosphate-buffered saline (PBS) and then detached with PBS containing 5 mM EDTA. ECM remaining on the plate was then solubilized with Triton X-100 and processed for Western blot.

For immunocytochemistry, cells were grown on glass cover slips at 1×10^3 cells per square centimeter in DMEM-F12 medium containing 10% FBS with 10 μM azacytidine for 3–5 days. Subsequently, cells were washed with PBS and fixed with 4% paraformaldehyde for 10 minutes. Cells were then permeabilized with 0.25% Triton X-100, 1% bovine serum albumin in PBS for 30 minutes at RT, and incubated overnight at 4°C with an anti-cardiac actin antibody and 4′,6-diamidino-2-phenylindole (DAPI) (Invitrogen). Cells were photographed after 2 or 5 days treatment with 5-azacytidine (5-aza).

Electron Microscopy

For electron microscopy studies, cells were detached with trypsin, centrifuged, and then fixed for 30 minutes with 2.5% glutaraldehyde in Hank's balanced salts solution (pH 7.4). Afterward, cells were postfixed with buffered 1% osmium tetroxide in a cacodylate buffer for 1 hour and dehydrated in an acetone series. Samples were embedded into Durcupan resin (Sigma-Aldrich). Slices were prepared using a Leica microtome. The resulting preparations with stained mitochondria were counted and imaged on a transmission electron microscope (JEOL JEM 1010). Images were captured using a Sony digital camera.

Flow Cytometry

Cells were detached on ice with PBS plus 5 mM EDTA and incubated with fluorescein isothiocyanate/tetra-methyl rhodamine isothiocyanate preconjugated antibodies against surface molecules for 30 minutes at 4°C. Cells were then washed and fluorescent samples were analyzed in a FACSCalibur Flow

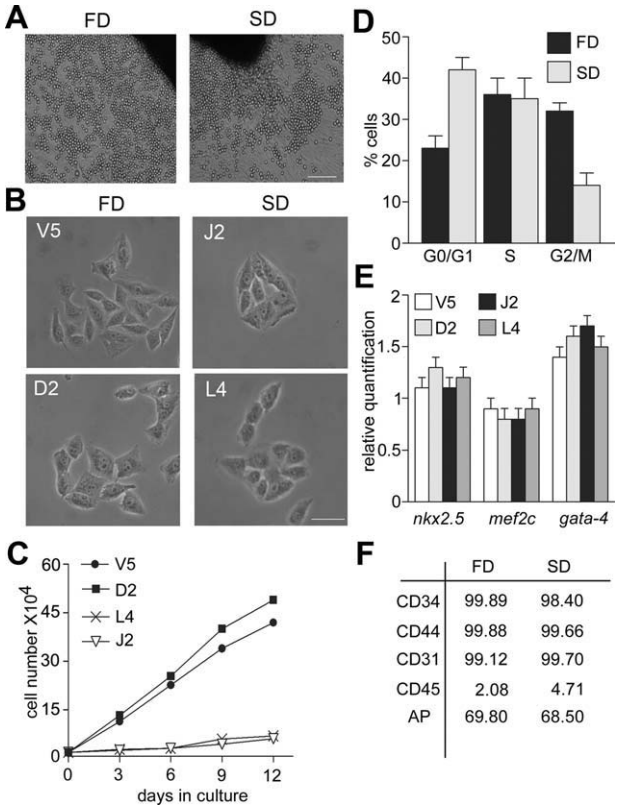

Figure 1. Characterization of mesoangioblast clones. **(A):** Cardiac mesoangioblasts isolated from heart explants. Scale bar = 100 μm. **(B):** Morphology of cardiac clones from fast dividing (FD) clones V5 and D2 and from slow dividing (SD) clones J2 and L4. Scale bar = 50 μm. **(C):** Proliferation of FD (V5 and D2) and SD (J2 and L4) clones. Graph represents the mean of four independent experiments. **(D):** Cell cycle analysis for FD and SD populations. Graph is representative of three independent experiments. **(E):** Quantitative reverse-transcription polymerase chain reaction analysis of *nkx2.5*, *mef2c*, and *gata-4* expression in SD (J2 and L4) and FD (V5 and D2) cell clones ($n = 4$). **(F):** Flow cytometry analysis of surface marker expression in FD and SD populations ($n = 3$). Abbreviations: AP, alkaline phosphatase; FD, fast dividing; G0, G0 phase; G1, G1 phase; M, M phase; S, S phase; SD, slow dividing.

cytometer. At least 10,000 events for each sample were counted. For analysis of mitochondrial mass, cells were harvested with 2 mM EDTA solution in PBS and washed with PBS. Mitochondrial mass was determined by staining the cells with 1 μM MitoTracker Green FM (Invitrogen), with 100 nM TMRM (Invitrogen), or with 100 nM JC-1 (Invitrogen) for 15 minutes at 37°C. Absorption of MitoTracker Green FM, TMRM, and JC-1 was determined by fluorescence-activated cell sorting (FACS) analysis. The uptake of MitoTracker (FL1) was used as an indicator for the mitochondrial mass, TMRM (FL2) staining was used as indicator for membrane potential and JC-1 (FL1 and FL2; only FL2 is shown) staining was used as an independent indicator of membrane potential. For each sample, at least 30,000 cells were analyzed for the corresponding fluorescence on a FACSCalibur Flow cytometer. Experiments were performed three times with similar results and polarization controls with cells incubated with the uncoupler carbonyl cyanide p-trifluoromethoxyphenylhydrazone (10 μM) were used to corroborate the function of the probes.

Modification of Mitochondrial Number

Mitochondria elimination in cells was induced with the addition of the respiratory chain inhibitor antimycin A (AM) (2 μM) and the uncoupler dinitrophenol (DNP) (400 μM) to cultures for 24 hours [18]. Cells were also treated with 20 mg/ml chloramphenicol (Chl) for 4 days to reduce the number of mitochondria. Mitochondrial morphology was analyzed by immunofluorescence [19]. The quantity of mitochondria was increased with the nitric oxide (NO) donors S-nitrosoacetyl penicillamine (SNAP, 100 μM) or diethylenetriamine (DETA)-NO (300 μM) for 24 hours as described previously [20]. Addition of reagents did not affect cell viability (Supporting Information Fig. S1). Mesoangioblasts were grown on cover slips, and mitochondria were stained with 200 nM MitoTracker Red FM or Green FM (Invitrogen). DAPI was used to stain nuclei. Cells were photographed under a Nikon microscope.

Measurement of Respiration and Acidification Rates

Oxygen consumption and acidification rates were measured in cells using a Seahorse XF-24 analyzer (SeahorseBioscience, North Billerica, MA www.seahorsebio.com). SD and FD cells were seeded in cell culture microplates at 30,000 cells per well in 200 μl growth medium and then incubated at 37°C for 12 hours. Assays were initiated by removing the growth medium and replacing it with 200 μl of assay medium (a low-buffered Roswell Park Memorial Institute medium with 1 mM phosphate) prewarmed to 37°C. The cells were incubated at 37°C for 30 minutes to allow media temperature and pH to reach equilibrium. Following equilibration, oxygen consumption rate (OCR) in picomoles per minutes (indicator of mitochondrial respiration) and extracellular acidification rate (ECAR) in milli-pH units per minutes (indicator of lactic acid production or glycolysis) were measured simultaneously for 2 minutes to establish a baseline rate. After baseline measurement, 80 μl of a testing agent prepared in assay medium was then injected into each well to reach the desired final concentration (Port A with 260 μM DNP, mitochondrial respiration uncoupler or with 5 μM oligomycin; and Port B with 400 mM potassium cyanide, complex IV inhibitor). New OCR and ECAR values were then determined. Two baseline rates and two response rates were measured and the average of two baseline rates or test rates was used for data analysis. At the end of the assay cells were detached with trypsin and the number and percentage of viable cells were determined after trypan blue exclusion using ViCell (Beckman-Coulter, Krefeld, Germany, www.beckmancoulter.com). Cell viability of all treated samples was similar when compared with control cells in acute assays lasting 1 hour.

Results

Characterization of Cardiac Mesoangioblasts Clones

Cardiac mesoangioblasts were obtained as described previously [7, 17]. In brief, hearts were collected from 4-week-old mice and the ventricles were isolated using a dissecting microscope. Recovered ventricles were further dissected into small fragments followed by plating into 1% gelatin-coated tissue culture dishes containing DMEM/20% serum (Fig. 1A). After 10 days, floating cells were collected and single clones were obtained by limiting dilution on gelatin-coated plates. All recovered clones acquired a characteristic triangular and refractile morphology at low density similar to as described previously (Fig. 1B; [7]). Interestingly, although morphologically identical, independent clones could be categorized by their proliferation potential in culture and were termed SD or FD. As illustrated in Figure 1C, two independent SD clones (J2 and L4), which represented about 90% of the total clones obtained, exhibited a doubling time of >72 hours in culture.

In contrast, approximately 10% of the total clones analyzed were FD populations, exemplified by the independent clones V5 and D2. These clones displayed a doubling time of approximately 24 hours in culture (Fig. 1C). Despite these differences in growth rates, all clones proliferated until passage 25, where they stopped dividing. This disparity in proliferation was mirrored by differences in the cell cycle of the two populations. In contrast to the FD population, higher numbers of SD cells were found in the G0/G1 phase of the cell cycle and fewer SD cells were at the G2/M phase, consistent with their observed slower growth rates (Fig. 1D). Gene expression analysis confirmed that both SD and FD cell types expressed the early cardiac transcription factors *Nkx2.5*, *Mef2c*, and *Gata4* (Fig. 1E) and were therefore deemed precommitted to the cardiac lineage. Further characterization of SD and FD clones revealed that both types stained positive for the surface markers CD31, CD34, CD44, and AP and were negative for CD45 (Fig. 1F), indicating a mesoangioblast phenotype [7]. Thus, these results suggested that two populations of cardiac mesoangioblasts could be isolated from ventricle explants with widely different proliferation rates.

Stimulation of Cardiac Mesoangioblast Differentiation

The ability of cardiac mesoangioblasts to undergo terminal differentiation was assessed with 5-aza, a DNA hypomethylating agent with proven utility in promoting cardiomyocyte differentiation from a range of ESCs and adult stem cells [7, 21, 22]. Accordingly, addition of 5-aza (10 μM) to the medium of SD cultures led to a progressive increase in the expression of the structural cardiac markers *α-actinin, connexin 43*, and *cardiac troponin* through 5 days in culture, as monitored by qRT-PCR (Fig. 2A). In contrast, parallel cultures of FD cells responded poorly to 5-aza treatment, with only minimal expression of mature cardiac markers throughout the time course (Fig. 2A). Furthermore, immunoblot analysis of 5-day-differentiated cells confirmed the expression of these cardiac structural protein in SD cells, which were clearly reduced in FD cells (Fig. 2B), and immunofluorescence for cardiac actin revealed strong sarcomeric staining in SD cells only (Fig. 2C). These results suggested that SD, but not FD, cells had the capacity to terminally differentiate to the cardiomyocyte lineage.

Mitochondria Abundance Correlates with Cell Differentiation

Increasing evidence suggest that mitochondria play important roles during the cellular differentiation of both lineage-restricted cells [23] and stem cells [13, 24]. In particular, stem cell commitment to the cardiac lineage appears strongly associated with mitochondrial metabolism [13, 14], with a concomitant decrease in proliferative capacity. Given this information, we next measured mitochondrial content in cardiac mesoangioblasts by a variety of methods. Using the mitochondria-selective dye, MitoTracker Green, confocal microscopy analysis of SD cells revealed a punctate staining pattern for mitochondria, which was significantly more intense than in FD cells stained in parallel (Fig. 2D). A similar result was obtained using MitoTracker Red (Supporting Information Fig. S2). Furthermore, FACS analysis showed that the overall mitochondrial abundance of SD clones was significantly higher than detected in FD cells (Fig. 2E, top). An additional mitochondrial marker, TMRM, that accumulates in cells in a membrane potential-dependent manner produced similar results (Fig. 2E, middle). Finally, JC-1, a ratiometric marker that also measures mitochondrial membrane potential in the SD population (Fig. 2E, bottom). To further show changes in mitochondrial abundance other methodologies were used. Immunoblotting of total cellular extracts revealed a slight increase in mitochondrial protein abundance in SD cells (Fig. 2F). These findings were extended by measurement of mitochondrial *mtDNA* content by qRT-PCR analysis, resulting in a *mtDNA*/*nDNA* ratio more than threefold higher in SD cells when compared with FD cells (Fig. 2G). Finally, electron microscopy was used to visualize intact mitochondria in both FD and SD populations, illustrating an approximately three- to fourfold increase in the number of mitochondria in SD cells when compared with FD cells (Fig. 2H). No differences in mitochondrial structure could be observed between the two populations. Collectively, these results indicated that, in contrast to FD cells, SD clones contained larger numbers of mitochondria, together with a greater capacity to undergo terminal differentiation to cardiomyocytes.

Oxygen Consumption Differs Between FD and SD Cells

Questioning whether the differences in mitochondrial mass between FD and SD cells were functionally relevant, we next measured OCR and ECAR using the Seahorse flux analyzer platform. As shown in Figure 2I (and Supporting Information Fig. S3), oxygen consumption differed between the two cell populations, with FD cells having higher OCR values when compared with SD cells, both under basal conditions and after addition of the uncoupler DNP to stimulate maximal respiration. In contrast, ECAR values, as a measure of acidification, were found to be higher in SD cells when compared with FD cells in culture (Fig. 2I and Supporting Information Fig. S3). Interestingly, after treatment with 5-aza to promote differentiation, whereas OCR and ECAR values in FD cells remained unchanged, SD cells exhibited a twofold increase in oxygen consumption coupled with a concomitant decrease in the ECAR acidification rate (Fig. 2I and Supporting Information Fig. S3). Taken together these results suggested that although SD cells contained a higher number of mitochondria than FD cells, the mitochondrial component was not being used for oxygen consumption until cells were prompted to differentiate. As these results were contrary to our expectations, we explored these findings in more detail. To do this, we developed a cell growth regime whereby galactose replaced glucose as a carbon source, thus forcing cells to use oxidative phosphorylation (rather than glycolysis) for energy production. In contrast to control (glucose-grown) conditions, where OCR values of FD cells were approximately twofold higher than SD cells, the situation was reversed under conditions of galactose growth. Under these conditions OCR values of SD cells were approximately threefold higher than those obtained with FD cells (Supporting Information Fig. S4A, S4B). This finding was consistent with the results obtained with differentiating SD cells and would suggest that SD cells have a latent mitochondrial capacity that can be used when needed. Indeed, when both FD and SD cells were cultivated in glucose medium oligomycin, an oxidative phosphorylation inhibitor, failed to decrease OCR values, indicating that mitochondria were not producing ATP under these conditions. Interestingly, under conditions of galactose growth, both cell populations could now respond to oligomycin, as shown by a decrease in OCR values (Supporting Information Fig. S4).

Mitochondrial Augmentation Promotes Cardiac Differentiation

Previous studies have demonstrated that mitochondrial abundance in diverse cell types can be augmented by the signaling

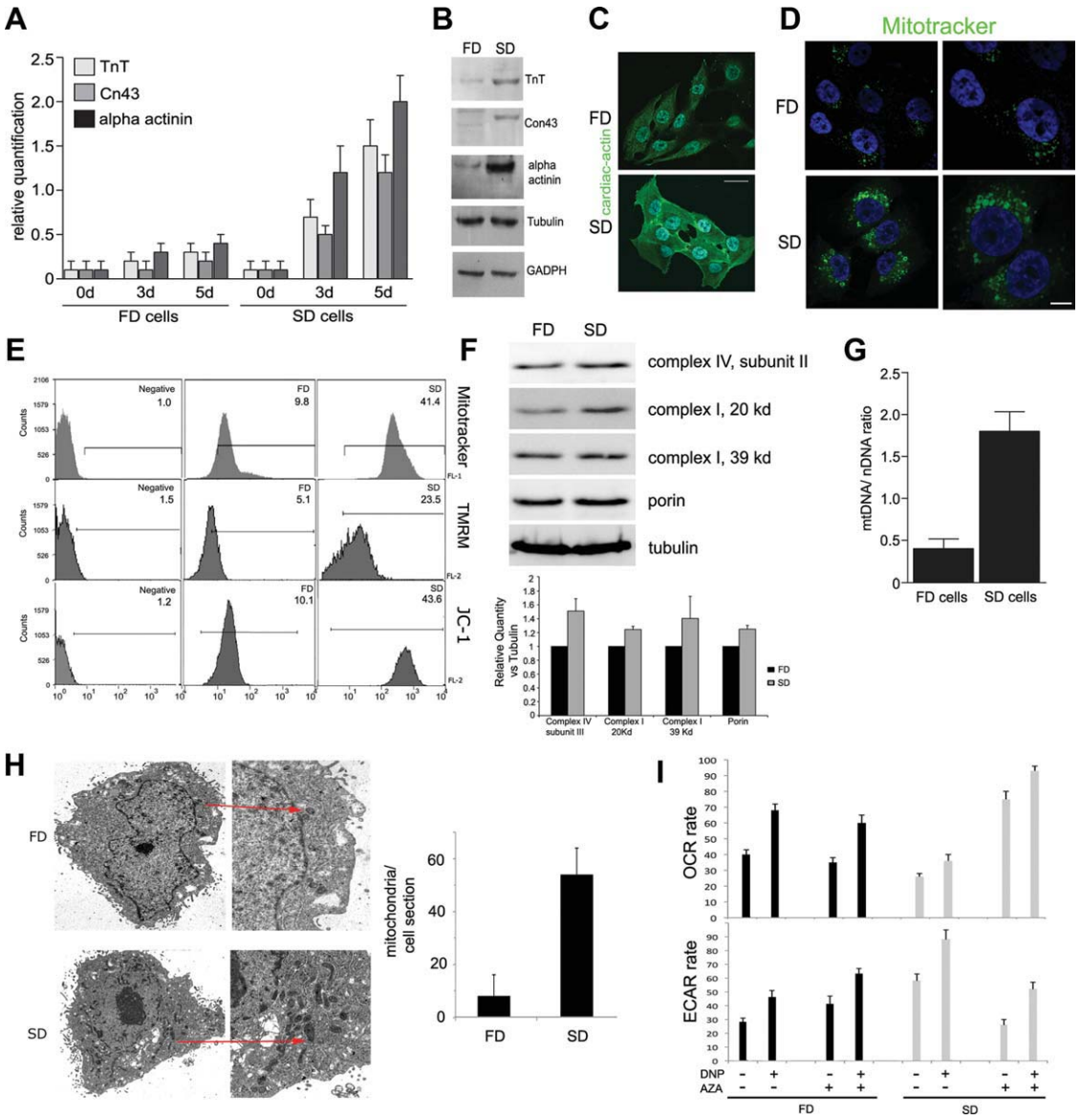

Figure 2. Mesoangioblast differentiation and mitochondrial quantification. **(A):** Quantitative reverse-transcription polymerase chain reaction (qRT-PCR) analysis of cardiac structural gene expression following 10 μM 5-azacytidine (5-aza) differentiation of fast dividing (FD) and slow dividing (SD) populations, ($n = 3$). **(B):** Western blot analysis of cardiac protein expression in FD and SD cells after 5-aza treatment for 5 days. Results are representative from two independent experiments. **(C):** Cardiac actin immunofluorescence of FD and SD clones after 5-aza treatment for 5 days. Scale bar = 100 μm. **(D):** Confocal microscopy of MitoTracker Green staining in FD clones (V5 and D2) and SD clones (J2 and L4). Scale bar = 50 μm. **(E):** Quantification of mitochondria in FD and SD clones by flow cytometry with MitoTracker Green, tetramethylrhodamine methyl ester, and JC-1 staining. One of three independent experiments is shown. Mean fluorescence intensity is shown at the upper right of the graphic. **(F):** Western blot analysis of mitochondrial protein expression in FD and SD clones. Tubulin was used as a cellular loading control. Results are representative from three independent experiments and protein quantification is shown in the graphic. **(G):** qRT-PCR analysis of mitochondrial DNA ratio in FD and SD cells, ($n = 3$). **(H):** Electron microscopy images of SD and FD clones (left panel with low ×8,000 magnification; right panel with high ×25,000 magnification). **(I):** Mitochondrial respiration rate and glycolysis (extracellular acidification rate) of SD and FD clones both in growing or differentiating conditions. Each data point represents mean ± SD ($n = 4$). Abbreviations: 5-Aza, 5-azacytidine; Cn43, connexin 43; DNP, dinitrophenol; ECAR, extracellular acidification rate; FD, fast dividing; mtDNA, mitochondrial DNA; nDNA, nuclear DNA; OCR, oxygen consumption rate; SD, slow dividing; TMRM, tetramethylrhodamine methyl ester; TnT, troponin.

molecule NO [20, 25]. To determine whether mitochondrial load was associated with mesoangioblast differentiation, we first treated FD cells with the NO donors SNAP and DETA-NO and monitored mitochondrial content with Mitotracker Green. As expected, application of 100 μM SNAP or 300 μM DETA-NO to growing cultures of FD-V5 cells augmented mitochondrial numbers, as measured by flow cytometry (Fig. 3A and Supporting Information Fig. S5). Moreover, fluorescence microscopy revealed significantly greater staining in V5 cells after NO-donor treatment (Fig. 3B). These results were confirmed by measuring *mtDNA* content as before. As shown in Figure 3C, the *mtDNA*/*nDNA* content of FD cells was significantly increased following both NO supplementation regimes. Results obtained from electron microscopy analysis also corroborated this finding and showed that addition of NO donors increased mitochondrial content in FD cells (Supporting

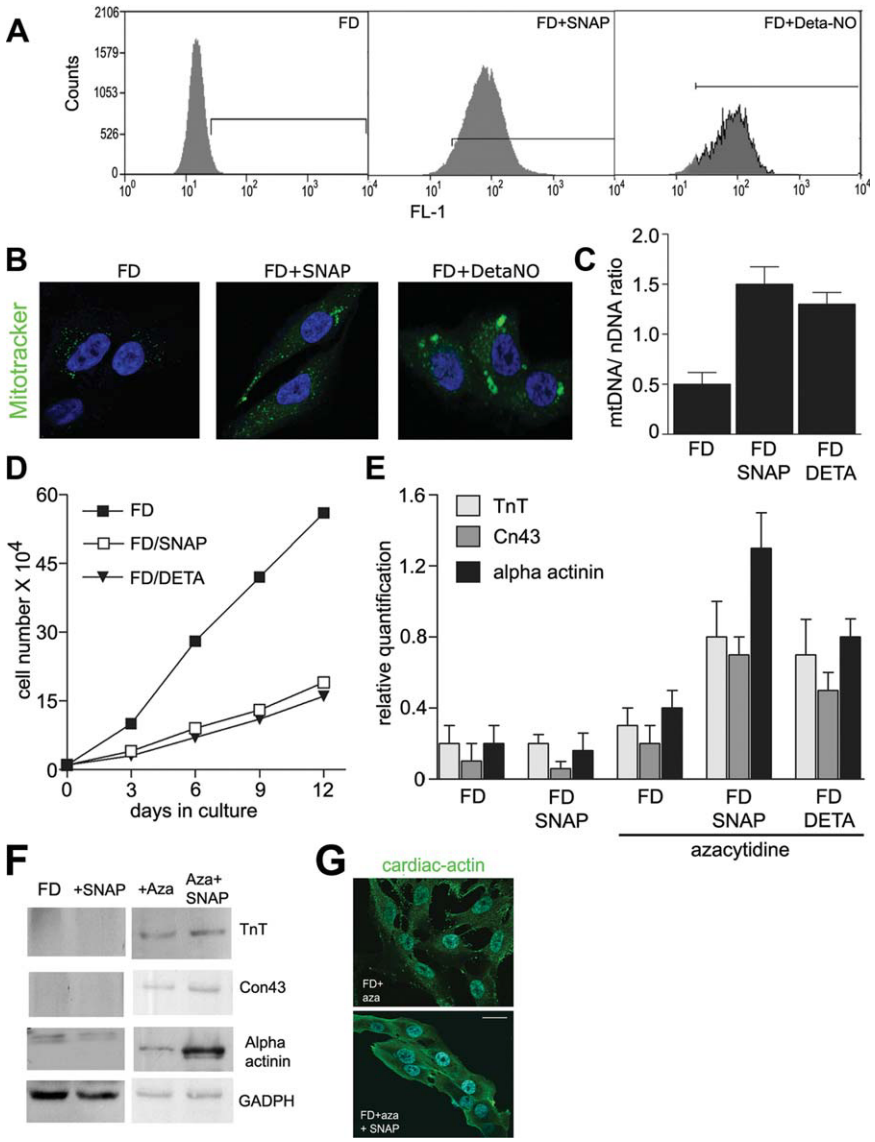

Figure 3. Nitric oxide (NO) modulates mitochondria number. **(A):** Fast dividing (FD) clone (V5) was treated or not with 100 μM S-nitrosoacetyl penicillamine (SNAP) or 300 μM Deta-NO for 24 hours and mitochondrial numbers were measured by flow cytometry using MitoTracker Green. One from three independent experiments is shown. **(B):** Confocal analysis of MitoTracker Green-stained cells after NO treatment (as above). **(C):** Quantitative reverse-transcription polymerase chain reaction (qRT-PCR) analysis of mitochondrial DNA content in FD cells after NO treatment, ($n = 4$). **(D):** Proliferation of FD clones during NO treatment. Graph represents the mean of three independent experiments. **(E):** qRT-PCR analysis of late cardiac gene expression in FD cells treated with SNAP (100 μM) with or without 5-azacytidine treatment (5 days). Graph represents the mean of three independent experiments. **(F):** Western blot analysis of cardiac protein expression after differentiation with 5-aza and SNAP treatment. **(G):** Immunofluorescence of cardiac actin expression in FD cells after treatment with 5-aza and SNAP. Scale bar = 50 μm. Abbreviations: Aza, 5-azacytidine; Cn43, connexin 43; DETA, diethylenetriamine; FD, fast dividing; NO, nitric oxide; SNAP, S-nitrosoacetyl penicillamine; mtDNA, mitochondrial DNA; nDNA, nuclear DNA; TnT, troponin.

Information Fig. S6). Notably, the increase in mitochondrial numbers in FD-V5 cells was associated with a decrease in their proliferation rate (Fig. 3D), to that observed in SD cells (Fig. 1C). At the same time, oxygen consumption analysis of FD cells treated for 24 hours with 100 μM SNAP revealed a decrease in OCR values to a similar rate found in SD cells (Supporting Information Fig. S4A). Moreover, when growth medium was switched from glucose to galactose, NO-treated FD cells had twofold higher OCR values than control conditions (Supporting Information Fig. S4B).

Remarkably, in contrast to control conditions, NO-treated FD cells had a significantly improved ability for cardiomyocyte differentiation upon addition of 5-aza to the culture medium, as demonstrated by increased gene expression of late cardiac markers (Fig. 3E), greater steady-state levels of cardiac proteins (Fig. 3F), and an abundance of well-defined sarcomeric cardiac actin structures (Fig. 3G). Importantly, the application of an NO-donor alone, to FD cells, was insufficient for differentiation (Fig. 3F). This is in contrast to the situation with ESCs, where spontaneous cardiac differentiation can be augmented with NO donors [26, 27]. In summary, these results strongly suggest that a combination of increased mitochondrial abundance, together with a permissive differentiation regime, is required for cardiac mesoangioblast differentiation.

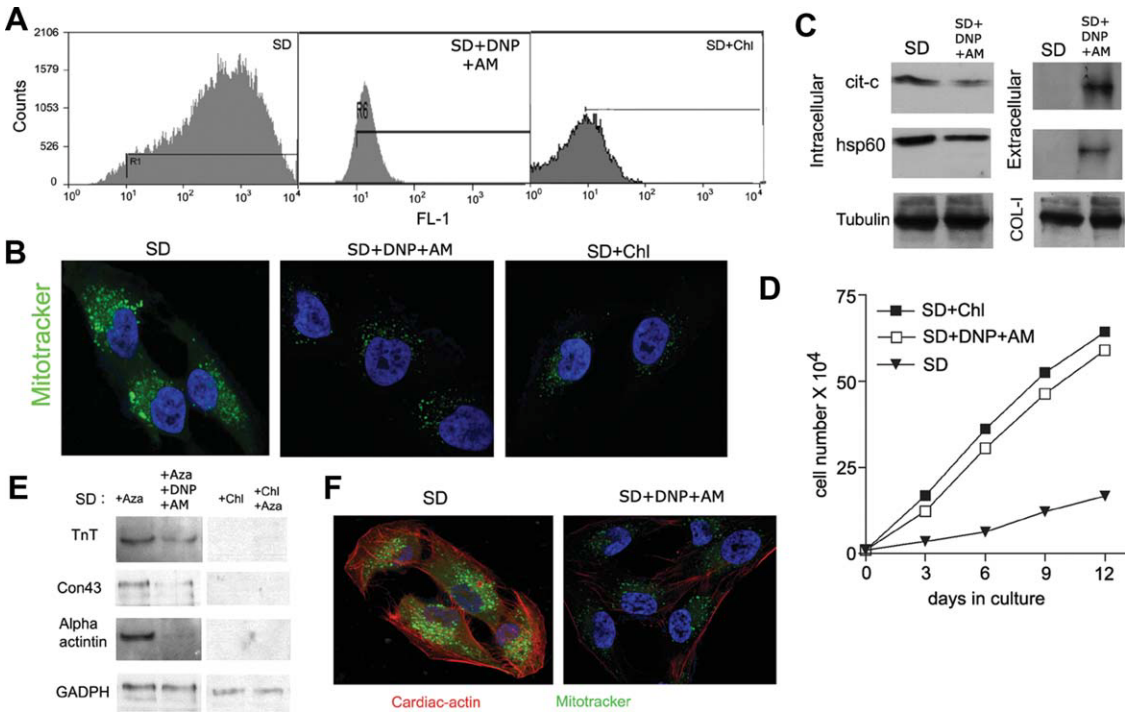

Figure 4. Mitochondrial loss inhibits cardiac differentiation. **(A):** SD cells were incubated with 0.4 mM DNP and 2 μM AM for 24 hours, or alternatively with 20 mg/ml Chl for 3 days. Cells were then stained with MitoTracker Green and mitochondrial number was measured by flow cytometry. One out of three independent experiments is shown. **(B):** Confocal analysis of Mitotracker Green-stained cells after treatment (as above). Bar, 100 μm. **(C):** Western blot analysis of mitochondrial protein expression after DNP/AM treatment. Tubulin was used to control for cell loading (intracellular), and COL-I was used to control for extracellular content. **(D):** Proliferation of SD cells during treatment with DNP/AM, or Chl, mean of three independent experiments. **(E):** Western blot analysis of cardiac protein expression in SD cells after 5-azacytidine (5-aza) differentiation with or without prior treatment with DNP/AM, or Chl. **(F):** Confocal microscopy analysis of cardiac actin immunofluorescence together with MitoTracker Green staining in fast dividing cells after treatment with 5-aza. Bar, 50 μm. Abbreviations: AM, antimycin A; Chl, chloramphenicol; cit-c, c-cytochrome; DNP, dinitrophenol; hsp60, heat shock protein 60; SD, slow dividing; TnT, troponin.

Loss of Mitochondria Abrogates Mesoangioblast Differentiation

Having shown that incrementing mitochondrial number in FD cells favored differentiation, we next questioned whether reducing mitochondrial abundance would impede cardiomyocyte differentiation in SD cells. To test this hypothesis, SD cells were treated with DNP and AM, a combination of mitochondrial poisons that induces mitochondrial elimination, coined mitoptosis [18, 28]. As an experimental control for mitochondrial diminution, SD cells were cultured with Chl, an inhibitor of mitochondrial protein synthesis [19]. As expected, SD cells treated with 400 μM DNP/2 μM AM for 24 hours, or alternatively, cultured with 20 mg/ml Chl for 4 days, had reduced numbers of mitochondria as measured by flow cytometry (Fig. 4A and Supporting Information Fig. S5), fluorescence microscopy (Fig. 4B), and electron microscopy (Supporting Information Fig. S6) Furthermore, FD cells undergoing mitoptosis contained reduced steady-state levels of intracellular mitochondrial proteins (cytochrome c and hsp60), together with an increased level of mitochondrial protein in the ECM (Fig. 4C) signifying mitochondrial extrusion. Intriguingly, this reduction in mitochondrial number, either through mitoptosis or through inhibition of mitochondrial biogenesis, led to an increased proliferation of SD cells to a rate similar to FD cells in culture (Fig. 4D). As anticipated, the reduction of mitochondrial number in SD cells led to an increase in OCR values in glucose medium (Supporting Information Fig. S4A) and, conversely, reduced OCR values in galactose medium (Supporting Information Fig. S4B). Consistent with our previous findings, 5-aza-treated SD cells, undergoing mitoptosis or inhibited for mitochondrial protein synthesis, failed to differentiate to cardiomyocytes as measured by a reduction of cardiac structural protein-abundance (Fig. 4E) together with less defined staining of sarcomeric cardiac actin (Fig. 4F) when compared with control cultures. Collectively, these data support the notion that mitochondria are intrinsically associated with cardiac potential

Human Cardiac Mesoangioblasts and Mitochondria

Having established the importance of mitochondrial density in murine cardiac mesoangioblast differentiation, we wondered if a similar system was operating in human cells. Our prior work revealed that cardiac mesoangioblasts isolated from patients undergoing surgery for myocardial infarction differed in their cardiac potential when compared with cells isolated from patients with ventricular hypertrophy and were nonresponsive to 5-aza treatment [17]. As shown in Figure 5A, mesoangioblasts from the infarcted group (Group A, clones A3 and A13) were similar in appearance to mesoangioblasts isolated from hypertrophic patients (Group B, clones B7 and B9) with a refractile and triangular morphology. Nevertheless, MitoTracker Green staining of Group B cells demonstrated reduced mitochondrial load in comparison to Group A cells, as measured by flow cytometry (Fig. 5B) and also microscopy (Fig. 5C). Consistent with our results in murine cells, addition of the NO-donor SNAP to growing cultures of Group B

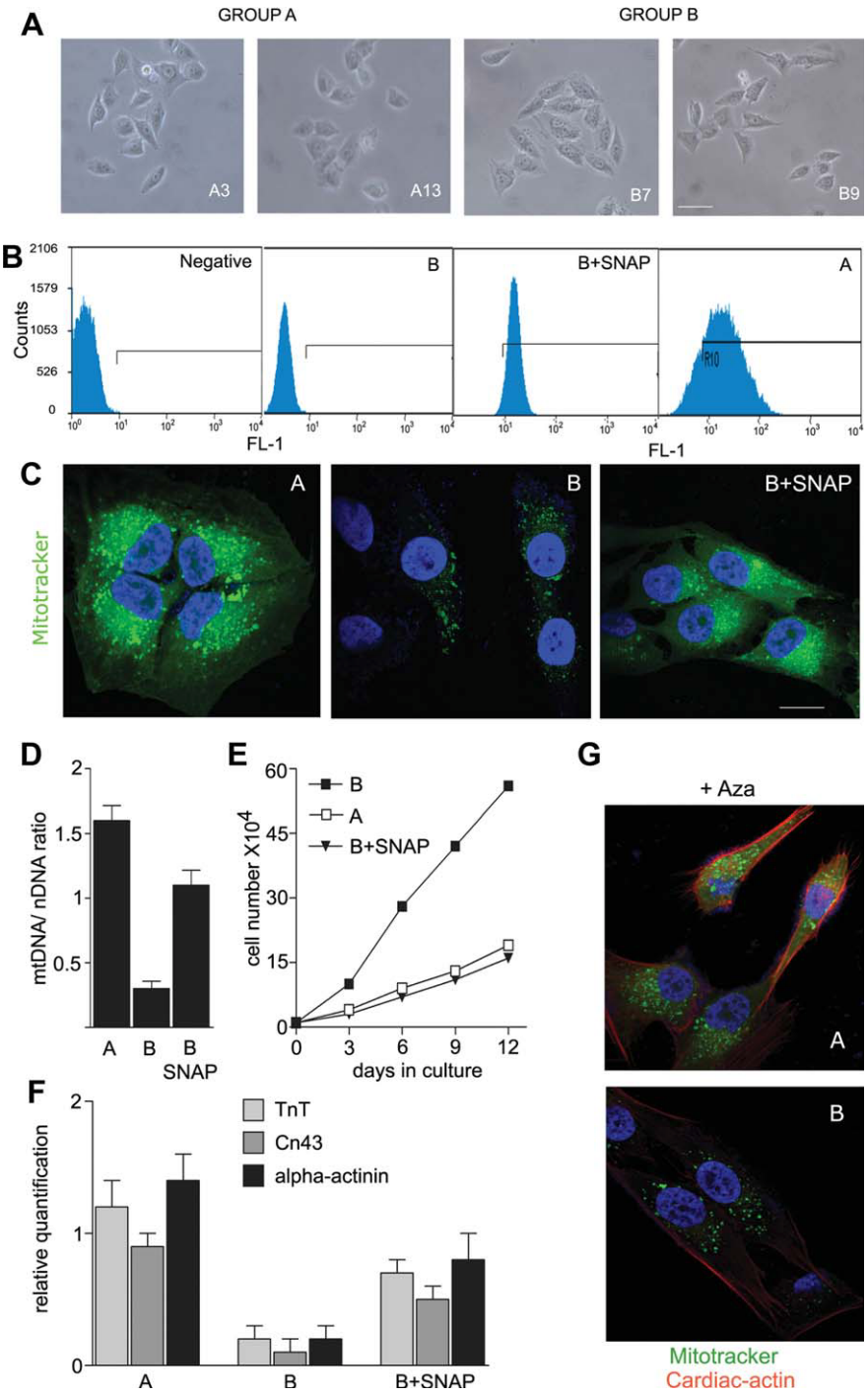

Figure 5. Characterization of human cardiac mesoangioblasts clones. **(A):** Morphology of cardiac clones from group A (A3 and A13) and group B (B7 and B9) patients. Scale bar = 50 μm. **(B):** Quantification of mitochondria number in group A and group B mesoangioblasts by flow cytometry, in the absence or presence of SNAP (100 μM, 24 hours). **(C):** Confocal microscopy of MitoTracker Green staining (as above). Scale bar = 100 μm. **(D):** Quantitative reverse-transcription polymerase chain reaction (qRT-PCR) analysis of mitochondrial DNA ratio in group B cells after nitric oxide treatment, (n = 4). **(E):** Proliferation rate of mesoangioblasts during SNAP treatment. (n = 4). **(F):** qRT-PCR analysis of late cardiac gene expression in the 5-aza–treated group A cells, group B cells, and group B cells pretreated with 100 μM SNAP. **(G):** Confocal microscopy analysis of cardiac actin immunofluorescence together with MitoTracker Green staining in group A and group B cells after treatment with 5-aza. Scale bar = 100 μm. Abbreviations: 5-aza, 5-azacytidine; *Cn43*, connexin 43; *mtDNA*, mitochondrial DNA; *nDNA*, nuclear DNA; SNAP, S-nitrosoacetyl penicillamine; *TnT*, troponin.

mesoangioblasts increased mitochondrial load (Fig. 5B, 5C) and, at the same time, increased the total ratio of mtDNA as measured by qRT-PCR (Fig. 5D). Notably, this increase in mitochondrial load in Group B cells after treatment with SNAP was associated with a reduced proliferation rate similar to the one of Group A (Fig. 5E). Importantly, the NO-induced greater number of mitochondria in Group B cells correlated with their increased ability to express cardiac structural

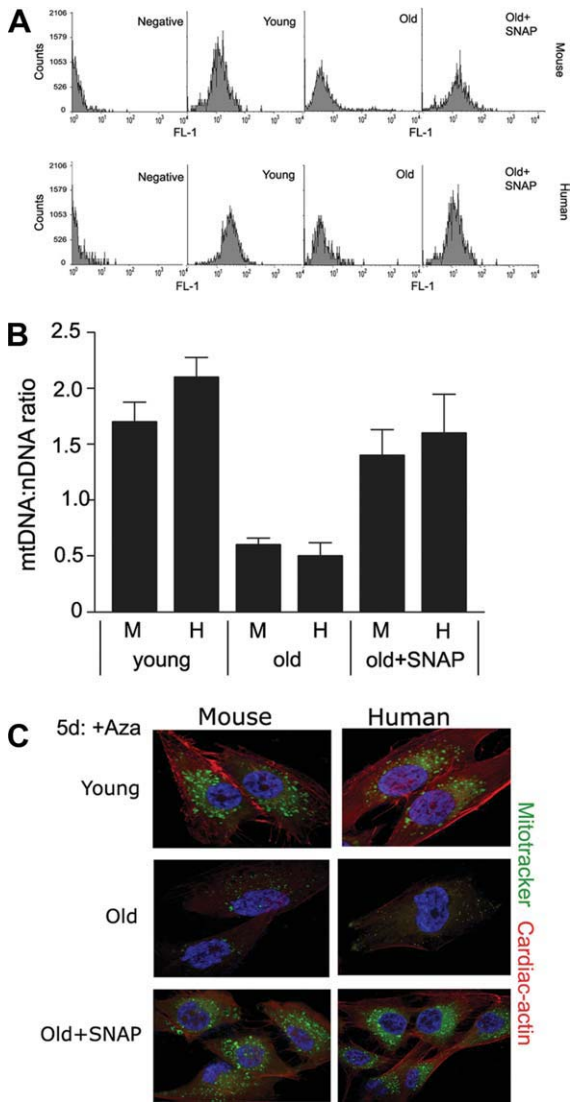

Figure 6. Aging and mitochondria. **(A):** Quantification of mitochondria number in young and old mesoangioblasts by flow cytometry, in the absence or presence of S-nitrosoacetyl penicillamine (100 μM, 24 hours). One of three independent experiments is shown. **(B):** Quantitative reverse-transcription polymerase chain reaction analysis of mitochondrial DNA ratio in young and old mesoangioblast cells after nitric oxide treatment, $n = 4$. **(C):** Confocal microscopy analysis of cardiac actin immunofluorescence together with MitoTracker Green staining in group A and group B cells after treatment with 5-azacytidine. Scale bar = 100 μm. Abbreviations: H, human; M, mouse; *mtDNA*, mitochondrial DNA; *nDNA*, nuclear DNA; SNAP, S-nitrosoacetyl penicillamine.

markers, similarly to Group A, upon differentiation with 5-aza, when compared with Group B cells with lower mitochondrial number (Fig. 5F). Furthermore, Group A cells expressed the structural marker cardiac actin, which was absent in parallel Group B cultures (Fig. 5G). Therefore, these findings lead us to conclude that in both murine and human-derived cardiac mesoangioblasts, the potential for terminal cardiac differentiation appears dependent on mitochondrial density.

Effects of Aging on Cardiac Mesoangioblasts Differentiation

Previous studies have highlighted decreased mitochondrial activity and/or density as a possible contributing factor in the cellular aging process [29, 30]. To ascertain whether animal age could influence cardiac potential, we first assessed the number of mitochondria from heart explant-mesoangioblasts of mice at 8 months of age (old) and compared these levels to those obtained from mice at 2 months of age (young). Interestingly, we found that >90% of clones isolated from young mice revealed a robust staining with MitoTracker Green (Fig. 6A, top). This is in contrast to our results obtained from mesoangioblasts isolated from 4-month-old mice, where only 10% stained for mitochondria (Fig. 2). At the other extreme, all mesoangioblast clones isolated from aged mice (8 months) showed a decreased cellular number of mitochondria (Fig. 6A, top). Moreover, all young-isolated mesoangioblasts had significantly lower proliferation rates than mesoangioblasts isolated from older animals (results not shown). Extending these findings, we performed a similar analysis in cardiac patients and examined mitochondrial levels in mesoangioblasts derived from patients younger than 30 years of age ($n = 9$) and compared these levels to patients older than 60 years of age ($n = 12$). Analogous to our results with aged mice, we found that mesoangioblasts from young patients more readily stained for mitochondria than parallel cultures from older patients (Fig. 6A, bottom). As anticipated, addition of SNAP to growing cultures of mesoangioblasts could augment the number of mitochondria in both old mouse and old human samples (Fig. 6A, 6B), and at the same time, increase the ability of old clones to express cardiac actin upon differentiation with 5-aza (Fig. 6C).

Discussion

Increasing evidence supports the notion that multipotent progenitor cells can be harvested from a variety of adult developed tissue [31–33]. Our prior studies reported the isolation of a novel mesoangioblast population from postnatal heart, which exhibited spontaneous commitment to the cardiomyogenic lineage [7, 17]. Given that factors affecting the growth and differentiation of these progenitor cells could be harnessed for regenerative heart repair, we focused our attention on the in vitro characteristics of these cells. Through these studies, we provide here the first evidence that mitochondrial load is an important feature for successful differentiation of these adult stem cells to cardiomyocytes.

Using explant-culturing procedures, two mesoangioblast populations could be isolated from mouse and human heart tissue. Although both populations expressed identical mesoangioblast surface markers, and appeared precommitted to the cardiac lineage (by expressing early cardiac transcription factors), they differed drastically in their proliferation rate, allowing us to characterize these cells as either fast or SD mesoangioblasts. Closer inspection of these populations revealed that SD clones contained many more mitochondria and could differentiate to cardiomyocytes upon stimulation, whereas FD clones contained reduced numbers of mitochondria in comparison with SD cells and were unable to undergo 5-aza-stimulated differentiation. We believe these attributes are causally linked to mitochondrial load because (a) increasing mitochondrial quantity with NO in FD cells resulted in a decrease in proliferation, together with an initiation of cardiac differentiation after 5-aza treatment and (b) decreasing the mitochondrial load in SD cells, by mitoptosis or Chl, increased cellular proliferation and also impeded cardiac differentiation. Thus, mitochondrial load was inversely proportional to proliferation and directly proportional to differentiation potential.

Remarkably, although mitochondrial load was dissimilar between SD and FD cells, oxygen consumption measurements did not reflect these differences and were actually the opposite to what was expected, at least under normal proliferation conditions in glucose supplemented media. However, when cells were forced to use oxidative phosphorylation for energy production by growth in galactose-supplemented medium, oxygen consumption then mirrored mitochondrial load. Of note, oligomycin-dependent respiration only occurred after growth in galactose, suggesting that ATP synthesis via respiration was not a major component for cell growth in glucose. Furthermore, oxygen consumption values increased during 5-aza treatment in SD cells implying that SD cells contain a reserve respiration capacity which may be required for differentiation. Overall, these results suggest that SD cell populations, by virtue of higher mitochondrial numbers, appear more adaptable than FD cells with regard to differentiation.

Reinforcing these findings, prior work has shown that osteogenic differentiation correlates with increased mitochondrial biogenesis in human mesenchymal stem cells [34] and mitochondrial defects limit differentiation of hematopoietic progenitor cells [35]. The relationship between mitochondria and differentiated status is more strongly maintained in ESCs and iPSCs, where the rapidly dividing and undifferentiated state has been linked to low mitochondrial mass or immaturity [36–38]. Although recent data would suggest that oxidative phosphorylation is an important mechanism for ATP generation [39] and differentiation [40] in ESCs. These more recent results are consistent with our findings, at least for cell differentiation, although it should be emphasized that our cell populations are taken from adult tissue. It is also important to note that mitochondria may serve regulatory roles beyond their historical function as the cellular powerhouse, for example, by production of ROS [41].

Our data also point to the aging process as an important factor potentially affecting the differentiation capability of mesoangioblasts. We found that mesoangioblasts isolated from both aged mouse and human samples were almost exclusively of the FD phenotype and showed little potential for cardiac differentiation when exposed to 5-aza. Limited information is available regarding cardiac progenitor cell differentiation with regards to aging; however, natural aging has been shown, in vivo, to decrease the functional (but not the total) pool of cardiac stem cells, both in mice and humans [42, 43]. Given that the quality of cardiac stem cells is a fundamental parameter of their regenerative potential, it is tempting to speculate that modulation of mitochondrial quantity may have utility in maintaining this functional pool. Our future studies will be directed to examining this possibility.

Conclusion

In summary, this study illustrates that mitochondrial quantity in mesoangioblasts can have significant effects on their downstream potential for cardiac differentiation. Whether this phenomenon is particular to our progenitor cells or is germane to other cardiac stem cells requires further investigation. Nevertheless, it is evident that mitochondrial load could be used in a selection regime to purify the best candidates from a polyclonal population, for transplantation studies.

Acknowledgments

We thank Giulio Cossu and his laboratory for providing reagents. We also thank Jose Antonio Enriquez and his laboratory for helpful discussions and for assistance with mtDNA measurements and oxygen consumption experiments. This work was supported in part by grants from Heart Repair and the Ministerio de Ciencia e Innovación (MICINN): SAF2010-15239 (to B.G.G.) and SAF2009-07965 (to K.J.M.) and also by the 'Ramón y Cajal' program from MICINN (to B.G.G.). The CNIC is supported by the MICINN and the Pro-CNIC Foundation.

Disclosure of Potential Conflicts of Interest

The authors indicate no potential conflicts of interest.

References

1 Yamada S, Nelson TJ, Crespo-Diaz RJ et al. Embryonic stem cell therapy of heart failure in genetic cardiomyopathy. Stem Cells 2008; 26:2644–2653.
2 Koyanagi M, Iwasaki M, Rupp S et al. Sox2 transduction enhances cardiovascular repari capacity of blood-derived mesoangioblasts. Circ Res 2010;106:1290–1302.
3 Kane NM, Meloni M, Spencer HL et al. Derivation of endothelial cells from human embryonic stem cells by directed differentiation: Analysis of microRNA and angiogenesis in vitro and in vivo. Arterioscler Thromb Vasc Biol 2010;30:1389–1397.
4 Jumabay M, Zhang R, Yao Y et al. Spotaneously beating cardiomyocytes derived from white mature adipocytes. Cardiovasc Res 2010;85: 17–27.
5 Marban E, Cheng K. Heart to heart: The elusive mechanism of cell therapy. Circulation 2010;121:1981–1984.
6 Blin G, Nury D, Stefanovic S et al. A purified population of multipotent cardiovascular progenitors derived from primate pluripotent stem cells engrafts in postmyocardial infarcted nonhuman primates. J Clin Invest 2010;120:1125–1139.
7 Gálvez BG, Sampaolesi M, Barbuti A et al. Cardiac mesoangioblasts are committed, self-renewable progenitors, associated with small vessels of juvenile mouse ventricle. Cell Death Differ 2008;15: 1417–1428.
8 Zaruba MM, Soonpaa M, Reuter S et al. Cadiomyogenic potential of c-Kit(+)-expressing cells derived from neonatal and adult mouse hearts. Circulation 2010;121:1992–2000.
9 Urbanek K, Cesselli D, Rota M et al. Stem cell niches in the adult mouse heart. Proc Natl Acad Sci USA 2006;103:9226–9231.
10 Passier R, Van Laake LW, Mummery CL. Stem-cell-based therapy and lessons from the heart. Nature 2008;453:322–329.
11 Kurz FT, Aon MA, O'Rourke B et al. Spatio-temporal oscillations of individual mitochondria in cardiac myocytes reveal modulation of synchronized mitochondrial clusters. Proc Natl Acad Sci USA 2010; 107:14315–20.
12 Hattori F, Chen H, Yamashita H et al. Nongenetic method for purifying stem cell-derived cardiomyoyctes. Nature 2010;7:61–66.
13 Chung S, Dzeja PP, Faustino RS et al. Mitochondrial oxidative metabolism is required for the cardiac differentiation of stem cells. Nat Clin Pract Cardiovasc Med 2007;4 suppl 1:S60–S67.
14 Crespo FL, Sobrado VR, Gomez L et al. Mitochondrial reactive oxygen species mediate cardiomyocyte formation from embryonic stem cells in high glucose. Stem Cells 2010;28:1132–1142.
15 Spitkovsky D, Sasse P, Kolossov E et al. Activity of complex III of the mitochondrial electron transport chain is essential for early heart muscle cell differentiation. FASEB J 2004;18:1300–1302.
16 Buggisch M, Ateghang B, Ruhe C et al. Stimulation of ES-cell-derived cardiomyogenesis and neonatal cardiac cell proliferation by reactive oxygen species and NADPH oxidase. J Cell Sci 2007;120: 885–894.
17 Gálvez BG, Covarello D, Tolorenzi R et al. Human cardiac mesoangioblasts isolated from hypertrophic cardiomyopathies are greatly

reduced in proliferation and differentiation potency. Cardiovasc Res 2009;83:707–716.
18 Lyamzaev KG, Nepryakhina OK, Saprunova VB et al. Novel mechanism of elimination of malfunctioning mitochondria (mitoptosis): Formation of mitoptotic bodies and extrusion of mitochondrial material from the cell. Biochim Biophys Acta 2008;1777:817–825.
19 Lipton JH, WC M. Mitochondrial biogenesis in cultured mammalian cells. II. Mitochondrial protein and phospholipid synthesis in chloramphenicol-treated BHK-21 cells. Biochem Biophys Acta 1977;477: 273–287.
20 Nisoli E, Clementi E, Paolucci C et al. Mitochondrial biogenesis in mammals: The role of endogenous nitric oxide. Science 2003;299: 896–899.
21 Makino S, Fukuda K, Miyoshi S et al. Cardiomyocytes can be generated from marrow stromal cells in vitro. J Clin Invest 1999;103:697–705.
22 Xu C, Police S, Rao N et al. Characterization and enrichment of cardiomyocytes derived from human embryonic stem cells. Circ Res 2002;91:501–508.
23 Ziabreva I, Campbell G, Rist J et al. Injury and differentiation following inhibition of mitochondrial respiratory chain complex IV in rat oligodendrocytes. Glia 2010;58:1827–1827.
24 Rehman J. Empowering self-renewal and differentiation: The role of mitochondria in stem cells. J Mol Med 2010;88:981–986.
25 Carraway MS, Suliman HB, Jones WS et al. Erythropoietin activates mitochondrial biogenesis and couples red cell mass to mitochondrial mass in the heart. Circ Res 2010;106:1722–1730.
26 Kado M, Lee JK, Hidaka K et al. Paracrine factors of vascular endothelial cells facilitate cardiomyocyte differentiation of mouse embryonic stem cells. Biochem Biophys Res Commun 2008;377:413–418.
27 Mujoo K, Sharin VG, Bryan NS et al. Role of nitric oxide signaling components is differentiation of embryonic stem cells into myocardial cells. Proc Natl Acad Sci USA 2008;105:18924–18929.
28 Cereghetti GM, Scorrano L. The many shapes of mitochondrial death. Oncogene 2006;25:4717–4724.
29 Safdar A, Hamadeh MJ, Kaczor JJ et al. Aberrant mitochondrial homeostasis in the skeletal muscle of sedentary older adults. PLoS One 2010;24:5:e10778.
30 Mammucari C, Rizzuto R. Signalling pathways in mitochondrial dysfunction and aging. Mech Ageing Dev 2010;131:536–543.
31 Katsumoto K, Shiraki N, Miki R et al. Embryonic and adult stem cell systems in mammals: Ontology and regulation. Dev Growth Differ 2010;52:115–129.
32 Bollini S, Smart N, Riley PR. Resident cardiac progenitor cells: At the heart of regeneration. J Mol Cell Cardiol 2011;50:296–303.
33 Riazi AM, Kwon SY, Stanford WL. Stem cell sources for regenerative medicine. Methods Mol Biol 2009;482:55–90.
34 Chen CT, Shih YR, Kuo TK et al. Coordinated changes of mitochondrial biogenesis and antioxidant enzymes during osteogenic differentiation of human mesenchymal stem cells. Stem Cells 2008;26: 960–968.
35 Inoue S, Noda S, Kashima K et al. Mitochondrial respiration defects modulate differentiation but not proliferation of hematopoietic stem and progenitor cells. FEBS Lett 2010;584:3402–3409.
36 Facucho-Oliveira JM, St John JC. The relationship between pluripotency and mitochondrial DNA proliferation during early embryo development and embryonic stem cell differentiation. Stem Cell Rev 2009;5:140–158.
37 Cho YM, Kwon S, Pak YK et al. Dynamic changes in mitochondrial biogenesis and antioxidant enzymes during the spontaneous differentiation of human embryonic stem cells. Biochem Biophys Res Commun 2006;348:1472–1478.
38 Prigione A, Fauler B, Lurz R et al. The senescence-related mitochondrial/oxidative stress pathway is repressed in human induced pluripotent stem cells. Stem Cells 2010;28:721–733.
39 Birket MJ, Orr AL, Gerencser AA et al. A reduction in ATP demand and mitochondrial activity with neural differentiation of human embryonic stem cells. J Cell Sci 2011;124:348–358.
40 Mandal S, Lindgren AG, Srivastava AS et al. Mitochondrial function controls proliferation and early differentiation potential of embryonic stem cells. Stem Cells 2010;29:486–95.
41 Droge W. Free radicals in the physiological control of cell function. Physiol Rev 2002;82:47–95.
42 Torella D, Rota M, Nurzynska D et al. Cardiac stem cell and myocyte aging, heart failure, and insulin-like growth factor-1 overexpression. Circ Res 2004;94:514–524.
43 Chimenti C, Kajstura J, Torella D et al. Senescence and death of primitive cells and myocytes lead to premature cardiac aging and heart failure. Circ Res 2003;93:604–613.

See www.StemCells.com for supporting information available online.